

Magnetic entropy change of $\text{Pr}_{1-x}\text{Ca}_x\text{MnO}_3$ manganites ($0.2 \leq x \leq 0.95$)

M. S. Reis* and V. S. Amaral

Departamento de Física and CICECO, Universidade de Aveiro, 3810-193 Aveiro, Portugal

J. P. Araújo

Departamento de Física and IFIMUP, Universidade do Porto, 4169-007 Porto, Portugal

P. B. Tavares

Departamento de Química and CQ-VR, Universidade de Trás-os-Montes e Alto Douro, 5001-911 Vila Real, Portugal

A. M. Gomes

Lab. Baixas Temperaturas, Inst. de Física, UFRJ, 21941-972 Rio de Janeiro-RJ, CP68528, Brasil

I. S. Oliveira

Centro Brasileiro de Pesquisas Físicas, Rua Dr. Xavier Sigaud 150 Urca, 22290-180 Rio de Janeiro-RJ, Brasil

(Received 1 September 2004; revised manuscript received 6 January 2005; published 19 April 2005)

In the present work we analyze the magnetic entropy change ΔS_M of the $\text{Pr}_{1-x}\text{Ca}_x\text{MnO}_3$ manganites, for a wide range of Ca concentrations ($0.20 \leq x \leq 0.95$). The results for the samples with $0.20 < x \leq 0.30$ present the usual behavior expected for ferromagnetic systems, peaking at the Curie temperature T_C . In contrast, for the charge-ordered antiferromagnetic samples ($0.30 < x < 0.90$), an anomalous magnetic entropy change starts around the charge-ordering temperature T_{CO} , persisting for lower values of temperature. This effect is associated to a positive contribution to the magnetic entropy change due to the charge-ordering ΔS_{CO} , which is superimposed to the negative contribution from the spin-ordering ΔS_{spin} ; that is described using a mean-field approximation. Supposing these contributions, we could also appraise ΔS_{CO}^{max} as a function of Ca content, which vanishes for the limits $x \sim 0.30$ and 0.90 and presents a deep minimum around $x \sim 0.50$, with two maxima at $x \sim 0.35$ and 0.65 . We conclude that for $x > 0.65$ only the magnetic order governs the charge ordering, contrarily to $x < 0.65$, where there are more than one mechanism ruling the charge ordering. Moreover, for the samples with phase coexistence ($0.30 < x \leq 0.40$), we found extremely large values for the magnetic entropy change at low temperatures. Finally, for $x > 0.90$, we found usual magnetic entropy change curves, peaking at the Néel temperature T_N .

DOI: 10.1103/PhysRevB.71.144413

PACS number(s): 75.30.Sg, 75.47.Lx, 75.47.Gk

I. INTRODUCTION

The magnetocaloric effect (MCE) is intrinsic to magnetic materials and is induced via coupling of the magnetic sublattice with the magnetic field, which alters the magnetic part of the total entropy due to a corresponding change of the magnetic field. The MCE can be estimated via the magnetic entropy change $\Delta S_M(T, \Delta H)$ and is a function of both temperature T and magnetic-field change ΔH , being usually recorded as a function of temperature, at a constant ΔH . In addition, the MCE has a significant technological importance, since magnetic materials with large values of $\Delta S_M(T, \Delta H)$ can be employed in various thermal devices.¹

The magnetic entropy is related to the magnetization M , magnetic field strength H , and absolute temperature T through the Maxwell relation²

$$\left[\frac{\partial S_M(T, H)}{\partial H} \right]_T = \left[\frac{\partial M(T, H)}{\partial T} \right]_H, \quad (1)$$

which after integration yields

$$\Delta S_M(T, \Delta H) = \int_{H_I}^{H_F} dS_M(T, H)_T = \int_{H_I}^{H_F} \left[\frac{\partial M(T, H)}{\partial T} \right]_H dH. \quad (2)$$

Hence, $\Delta S_M(T, \Delta H)$ can be numerically calculated using Eq. (2) and the measured magnetization as a function of magnetic field and temperature.

Several authors through many decades have studied the magnetocaloric effect in a large variety of magnetic materials. However, more recently, a large amount of work³⁻¹⁹ was devoted to explore the MCE in the mixed-valency manganites AMnO_3 , where A is a trivalent rare-earth mixed with a divalent alkaline earth. Among these referred works, some of them worked out the MCE around the charge-ordering temperature T_{CO} , however, only for systems in which the charge-ordered state arises below the Curie temperature ($T_C > T_{CO}$), as the case of Pr-Sr¹¹ and Nd-Sr⁴ manganites. On the other hand, the magnetic properties are very different for systems in which the charge-ordered phase arises in the paramagnetic regime ($T_N < T_{CO}$), as the case of Pr-Ca, Nd-Ca and Sm-Ca manganites,^{20,21} and, from the best of our knowledge, the MCE was never reported in this case, although

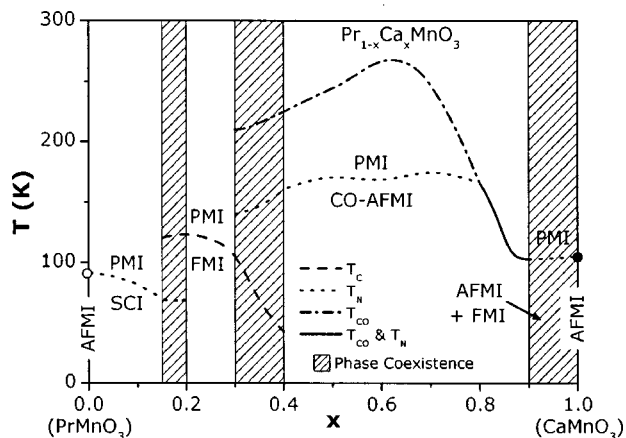


FIG. 1. Magnetic and electric phase diagram for $\text{Pr}_{1-x}\text{Ca}_x\text{MnO}_3$ manganites. PMI-paramagnetic insulator; SCI-spin-canted insulator; FMI-ferromagnetic insulator; CO-AFMI-charge-ordered antiferromagnetic insulator; AFMI-non-charge-ordered antiferromagnetic insulator. Open and closed circles represent PrMnO_3 and CaMnO_3 , respectively. Different lines denote different types of transitions.

there are several specific heat studies.²²⁻²⁴ In addition to the charge-ordering phenomena, several interesting features emerge for the $\text{Pr}_{1-x}\text{Ca}_x\text{MnO}_3$ manganites, series in which we will focus our attention.

Pure PrMnO_3 has an A-type antiferromagnetic-insulator AFMI arrangement, changing discontinuously to a spin-canted-insulator SCI structure with small amounts of Mn^{4+} dopant.²⁵ This SCI phase remains up to $x=0.20$, whereas for $0.20 < x \leq 0.30$ a ferromagnetic-insulator FMI phase arises, with Curie temperature around 120 K.²⁶⁻²⁹ Between $x=0.15$ and 0.20 , a phase coexistence takes place with SCI and FMI phases. For $0.30 < x < 0.90$, an AFMI phase establishes for temperatures typically below 170 K,^{26,27,30} coexisting with a charge-ordered CO state with onset temperature T_{CO} between 210 K, for $x \sim 0.30$, and 110 K, for $x=0.85$.²⁶ For $0.30 < x \leq 0.40$ a remarkable phase coexistence^{23,26-35} with FMI and CO-AFMI phases can be found. It is well established^{30,32,33} that the clusters embedded in the antiferromagnetic matrix achieve the ferromagnetic order around 110 K for $x \sim 0.30$, and 42 K for $x \sim 0.40$.²⁷ In this direction, our work using NMR³¹ gives the ferromagnetic fraction within the antiferromagnetic matrix, as a function of Ca content, x . For the Ca-rich samples $x \geq 0.90$, another strong phase coexistence arises, with ferromagnetic domains embedded in a non-charge-ordered AFMI matrix. For $x=0.90$ the ferromagnetic phase is stable, decreasing its volume fraction as the Ca content x increasing toward the unity, reaching the well-known G-type antiferromagnetic CaMnO_3 .³⁶ The phase diagram presented in Fig. 1 is slightly dependent on the sample preparation procedure. Discrepancies found in literature can be attributed to differences in grain sizes,^{13,37-39} oxygen contents,³⁹⁻⁴³ vacancies on the lattice,⁴⁴ etc. Additionally, the phase diagram presented here is not completely established, since the magnetic structure for several values of Ca concentration x is still a matter of discussion.^{23,26-29,32-35}

II. EXPERIMENTAL PROCEDURE

The samples with $x < 0.50$ were prepared by the ceramic route, starting from the stoichiometric amount of Pr_2O_3 (99.9%), CaCO_3 (>99%) and MnCO_3 (>99%), and heated in air, with five intermediate crushing (pressing) steps. On the other hand, for $x \geq 0.50$, we used the sol-gel method with urea, following the procedure described in Ref. 45. The final crushed powders were compressed and sintered in air at 1350 °C during 45 h (for the ceramic route) and 1300 °C during 60 h (for the sol-gel technique), with a subsequent fast freezing of the samples. X-ray diffraction patterns confirmed that the samples lie in the $Pbnm$ space group, without vestige of spurious phases.

The temperature and external magnetic field dependence of the magnetization were carried out using a commercial SQUID and PPMS magnetometers. The data were acquired after the sample had been zero-field cooled, under the isothermal regime (M versus H curves), varying the applied magnetic field from zero up to 4 T and temperature ranges from 10 K up to 300 K. After each M versus H curve, the sample was heated to the next temperature desired without the influence of the external magnetic field. For the dc susceptibility $\chi_{\text{dc}} (=M/H$ at low field), the measurements were performed at a fixed magnetic field, sweeping the temperature.

III. RESULTS

In this section we will describe the field and temperature dependence of the magnetization $M(T, H)$, since it is one of the best experimental tools to understand the magnetocaloric effect of the system under study. The zero-field-cooled (ZFC) and field-cooled (FC) dc susceptibilities χ_{dc} , were measured for all samples available ($x=0.20, 0.25, 0.30, 0.32, 0.35, 0.40, 0.45, 0.50, 0.55, 0.65, 0.70, 0.75$ and 0.95). We observed a similar behavior for those below the onset concentration for charge ordering ($x \sim 0.30$), with a well-defined transition from the paramagnetic to the ferromagnetic phase. Although the dc susceptibility χ_{dc} , after field cooling increases with decreasing temperature, after the sample had been zero-field-cooled, it keeps an almost temperature-independent feature. Additionally, from the quantity $1/\chi_{\text{dc}}$, we could observe the usual Curie-Weiss law, allowing one to estimate the value of the paramagnetic effective moment p_{eff} and the paramagnetic Curie temperature θ_p . Thus, Fig. 2(a) presents the behavior described above, representative for all samples $x \leq 0.30$. On the other hand, for $0.30 < x < 0.90$, the dc susceptibility presents a maximum around T_{CO} and a well-defined transition from the paramagnetic to the antiferromagnetic phase. For the samples with phase coexistence ($0.30 < x \leq 0.40$), the maximum amount of FMI phase allowed to be in the system occurs at T_0 , also observed [see Fig. 2(b)]. In our recent publication,⁴⁶ we discuss in details the meaning of T_0 , as well as the influence of the phase coexistence on the magnetic entropy change. Finally, the charge-ordering feature completely disappears for $x > 0.90$, as presented in Fig. 2(c). The quantities obtained from the analysis of the dc susceptibility are summarized in Table I. In addition, note the

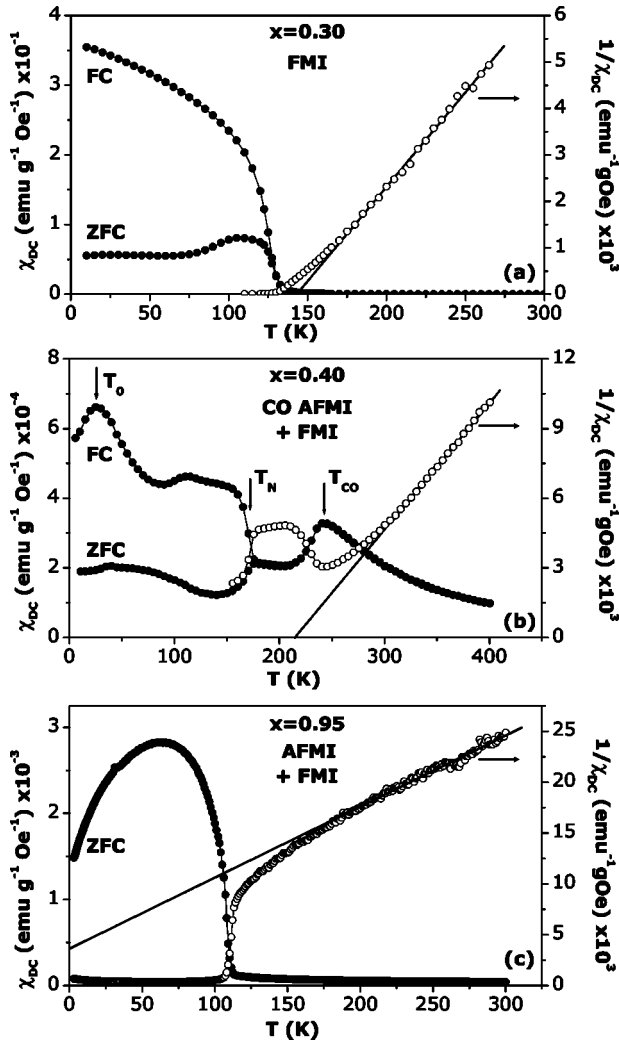


FIG. 2. Left axis: zero-field-cooled (ZFC) and field-cooled (FC) dc susceptibility χ_{dc} ($=M/H$ at low field) as a function of temperature, for (a) $x=0.30$, (b) $x=0.40$, and (c) $x=0.95$. Right axis: temperature dependence of the inverse of the dc susceptibility.

ferromagnetic fluctuations that arise in the paramagnetic phase of the CO-AFMI samples ($0.30 < x < 0.90$), since their paramagnetic Curie temperatures θ_p are positive. Nevertheless, the asymptotic paramagnetic Curie temperature shifts gradually toward negative temperatures, reaching -52 K for $x=0.95$, even with the small amount of ferromagnetic phase (expected to be found for $x > 0.90$).²⁵

The temperature and field dependence of the magnetization $M(T, H)$ were also measured for all samples. From the data analysis of several M versus H isotherms, we could build the curves for the thermal dependence of the magnetization, at a fixed magnetic field. For $x=0.20$, decreasing temperature, one observes that the magnetization starts to increase faster below 100 K, peaking at around 35 K, as displayed in Fig. 3(a). It is related to the coexistence of SCI and FMI phases, for $0.15 \leq x \leq 0.20$ (see Fig. 1).^{25,27,28} On the other hand, for $x=0.25$ and 0.30 an usual ferromagnetic behavior for the thermal dependence of magnetization is found, as presented in the inset of Fig. 3(a). However, for Ca concentrations x within the phase coexistence region (0.30

TABLE I. Values obtained for: T_0 , related to the maximum amount of FMI phase allowed to be in the phase coexistent system ($0.30 < x \leq 0.40$);⁴⁶ T_{CO} , charge-ordering temperature; the critical temperature T_{crit} , obtained from the maximum of $d\chi_{dc}/dT$; θ_p , the paramagnetic Curie temperature; and, finally, p_{eff} , the paramagnetic effective moment.

x	T_0 (K)	T_{CO} (K)	T_{crit} (K) ^a	θ_p (K)	p_{eff} (μ_B)
0.20			94	110	7.0
0.25			119	137	5.6
0.30			125	143	5.0
0.32	26	210	113	180	4.9
0.35	19	222	178	211	4.3
0.40	11	239	176	215	4.3
0.45		244	165	270	4.2
0.50		242	140	266	4.2
0.55		252	145	262	4.2
0.65		274	150	254	4.0
0.70		256	94	191	3.9
0.75		205	104	141	4.1
0.95			108	-52	4.0

^a T_C for $x \leq 0.30$ and T_N for $x > 0.30$.

$< x \leq 0.40$), different features emerge. For $x=0.40$, for instance, we found two humps, around 239 and 176 K, corresponding to the establishment of the charge ordering and the antiferromagnetic spin ordering, respectively, in accordance with several works,^{27,28} including those using neutron diffraction.^{30,32,47,48} As the temperature is further decreased, we can verify a remarkable increasing of the magnetization also below 100 K, peaking at around $T_0=11$ K, with a subsequent loss of magnetic moment. This peak at low temperatures is also related to the phase coexistence present in this range of Ca concentration⁴⁶ (see Fig. 1). A similar behavior had been found for all samples with $0.30 < x \leq 0.40$. This feature, which can be seen in Fig. 3(b) and its inset, was already observed for $x=0.37$.²³ On the other hand, for $0.40 < x < 0.90$ [inset on Fig. 3(c)], we still found the charge ordering and Néel temperature, however, without the metamagnetic transition at low temperatures, since there is no more phase coexistence. For $x=0.95$ [Fig. 3(c)], a well-behaved curve arises with a defined transition from the paramagnetic to the non-charge-ordered AFMI phase.

Finally, Fig. 4 presents $M(H)$ curves at 4.2 K and $M(T)$ curves at 4 T, for $x=0.20, 0.25, 0.30$, and 0.32 . These curves confirm the phase diagram, which establishes a pure ferromagnetic phase for the samples with $0.20 < x \leq 0.30$.

IV. THE MAGNETOCALORIC EFFECT

In the previous sections, we provided detailed information referring to the magnetic properties of the $\text{Pr}_{1-x}\text{Ca}_x\text{MnO}_3$ manganites. The aim of the present section is the discussion of the magnetocaloric effect of these manganites obtained from the previously presented magnetic data.

Figure 5 presents the magnetic entropy change $\Delta S_M(T)$ for all samples studied ($x=0.20, 0.25, 0.30, 0.32, 0.35, 0.40$,

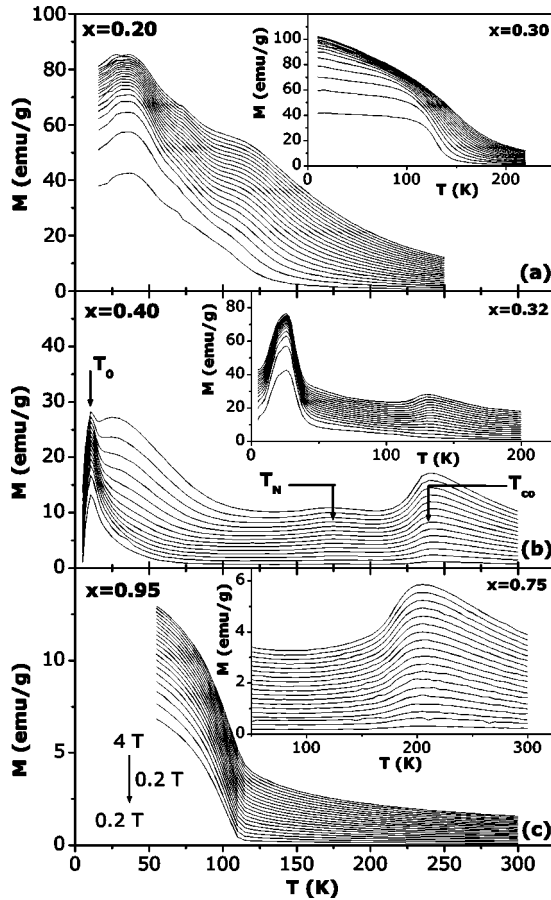


FIG. 3. Temperature dependence of the magnetization data for (a) $x \leq 0.30$, (b) $0.30 < x \leq 0.40$, and (c) $x > 0.40$. These graphics were built from the measured M vs H curves, for several temperatures.

0.45, 0.50, 0.55, 0.65, 0.70, 0.75, and 0.95), under 4 T of magnetic-field change. For $x=0.20$ [Fig. 5(a)], the magnetic entropy change has a usual behavior for temperatures above 100 K, where the magnetization data [Fig. 3(a)] has also a

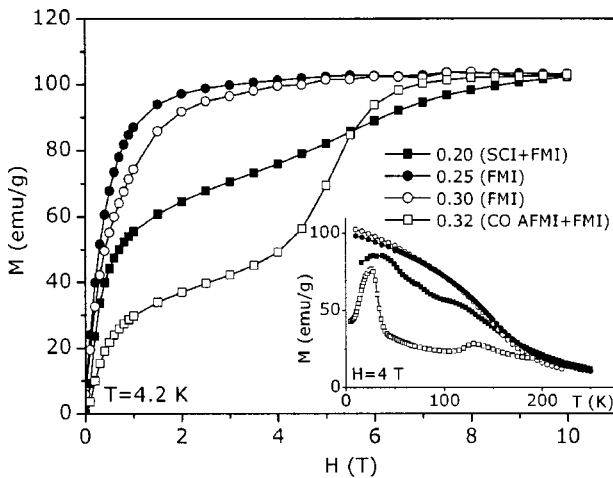


FIG. 4. Magnetization as a function of magnetic field, at 4.2 K, and temperature, at 4 T, for $x=0.20$ (SCI+FMI), 0.25 and 0.30 (FMI), and 0.32 (CO AFMI+FMI).

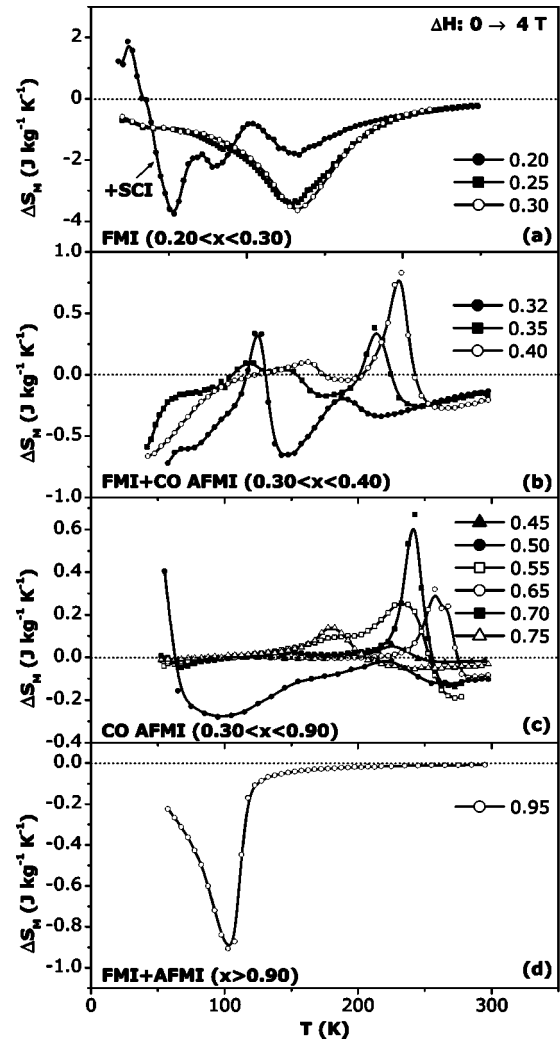


FIG. 5. Temperature dependence of the magnetic entropy change under 4 T of magnetic-field change for all samples available and covering all different magnetic phases of this $\text{Pr}_{1-x}\text{Ca}_x\text{MnO}_3$ series: FMI-ferromagnetic insulator; CO AFMI-charge-ordered antiferromagnetic insulator; AFMI-non-charge-ordered antiferromagnetic insulator.

well-shaped feature. However, below 100 K, the magnetization starts to increase faster as the temperature is further decreased, due to a SCI and FMI phase coexistence, as already discussed in the previous section. On the other hand, for $x=0.25$ and 0.30, concentrations completely embedded within the ferromagnetic region, we found an usual behavior for ΔS_M , as sketched in Fig. 5(a). We consider, in the case of $x=0.25$ and 0.30, that the contribution to the magnetic entropy change is purely due to the spin magnetic moments of the sample, since these concentrations have pure ferromagnetic phases (see Fig. 4). However, for the samples with $0.30 < x < 0.90$, the charge-ordering arrangement plays a decisive role. When the temperature is further decreased, the magnetic entropy change ΔS_M follows an usual shape until the charge-ordering temperature T_{CO} , below which such behavior is completely broken, as can be observed in Figs. 5(b) and 5(c). Finally, for $x=0.95$, the magnetic entropy change recovers the usual shape, as sketched in Fig. 5(d).

To analyze this intriguing and anomalous feature, which arises for $0.30 < x < 0.90$, some aspects should be taken into account. First of all, we consider two different contributions to the total magnetic entropy change ΔS_M : one refers to the spin rearrangement ΔS_{spin} , and the other concerns the charge-ordering rearrangement ΔS_{CO} , as follows:

$$\Delta S_M = \Delta S_{\text{spin}} + \Delta S_{\text{CO}}. \quad (3)$$

For $T_N < T < T_{\text{CO}}$, i.e., in the paramagnetic phase, an applied magnetic-field forces a rude alignment of the spins, increasing the Mn^{3+} - Mn^{4+} electron hopping and decreasing the concentration of Mn^{3+} - Mn^{4+} charge ordering, when compared to the zero-field case. Consequently, the entropy because of the CO increases under an external applied magnetic field, allowing a positive CO entropy change. On the other hand, for $T > T_{\text{CO}}$, there is no charge ordering, implying, of course, in a null CO entropy change. In addition, as described above, the paramagnetic phase of these samples has ferromagnetic fluctuations ($\theta_p > 0$, see Table I). Thus, we considered, as a first approximation, that ΔS_{spin} arises from a simple ferromagnetic mean-field interaction, at least around $T_{\text{CO}} (> T_N)$, i.e., in the paramagnetic phase. In this direction, the effective field can be written as

$$H_{\text{eff}} = H_{\text{ext}} + \lambda g J \mu_B B_J(x) \quad (4)$$

where H_{ext} stands for the external magnetic field, λ the mean-field parameter, $B_J(x)$ the Brillouin function, and

$$x = \frac{g J \mu_B H_{\text{eff}}}{k_B T} \quad (5)$$

Thus, from the Gibbs-Von Neumann entropy

$$S = -k_B \text{Tr} \{ \hat{\rho} \ln \hat{\rho} \} \quad (6)$$

is possible to obtain the magnetic entropy due to the spin ordering, in k_B units:

$$S_{\text{spin}}(T, H_{\text{ext}}) = \ln \left\{ \frac{\sinh \left[x \left(1 + \frac{1}{2J} \right) \right]}{\sinh \left[\frac{x}{2J} \right]} \right\} - x B_J(x), \quad (7)$$

where $\hat{\rho}$ is the density operator corresponding to a Hamiltonian $\hat{\mathcal{H}} = -\hat{\mu} \cdot \vec{H}$. Finally, the magnetic entropy change due to spin ordering can be written as

$$\Delta S_{\text{spin}}(T, \Delta H) = S_{\text{spin}}(T, H_{\text{ext}}) - S_{\text{spin}}(T, 0). \quad (8)$$

We know, from the high-temperature magnetic measurements, the paramagnetic Curie temperature θ_p and the paramagnetic effective moment p_{eff} (see Table I), and from the well-known relationships

$$p_{\text{eff}} = g \sqrt{J(J+1)} \quad (9)$$

$$\lambda = \frac{3k_B \theta_p}{p_{\text{eff}}^2} \quad (10)$$

that we can obtain the mean-field parameter λ and the total angular moment J . We considered $g=2$, since this value was

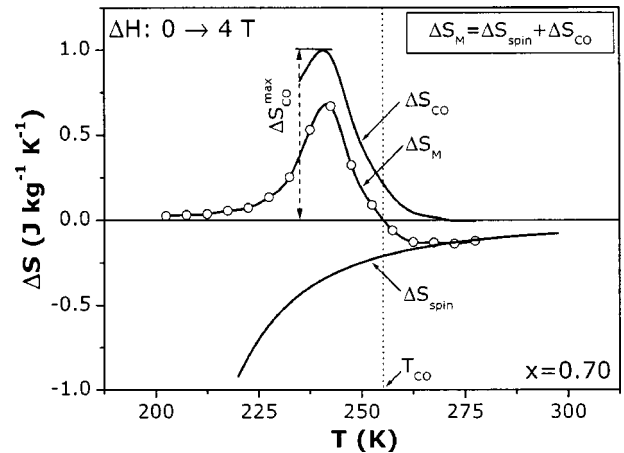


FIG. 6. Estimative of the charge-ordering contribution ΔS_{CO} to the total magnetic entropy change ΔS_M . See text for details concerning the spin contribution ΔS_{spin} [Eq. (8)].

already found for several manganites.^{49–51} Thus, using the measured λ and J , we estimated ΔS_{spin} [Eq. (8)], which exactly matches ΔS_M at high temperatures. Consequently, we could appraise $\Delta S_{\text{CO}}^{\text{max}}$, the value of charge-ordering contribution slightly below T_{CO} , i.e., around the maximum of ΔS_M , as drawn in Fig. 6, for $x=0.70$.

Following the procedure described above the concentration dependence of $\Delta S_{\text{CO}}^{\text{max}}$ could be built, vanishing for the limits $x \sim 0.30$ and 0.90 and presenting a deep minimum for $x \sim 0.50$, with two maxima around $x \sim 0.35$ and 0.65 , as shown in Fig. 7. These values are of the same order of those obtained for Nd—Sr manganites,⁴ around the charge-ordering temperature.

For $\text{Pr}_{1-x}\text{Ca}_x\text{MnO}_3$ manganites the charge-ordering entropy arises from the excess of Mn^{3+} or Mn^{4+} , depending on whether $x < 0.50$ or $x > 0.50$, respectively. Since there are $(1-2x)$ Mn^{3+} unpaired (for $x < 0.50$, for example) and such excess vanishes at $x=0.50$, it is expected that $\Delta S_{\text{CO}}^{\text{max}}$ has a deep minimum around $x=0.50$. On the other hand, the maximum at $x \sim 0.65$ can be understood via the analysis of ΔS_{spin} and ΔS_M as a function of the magnetic-field change ΔH , as

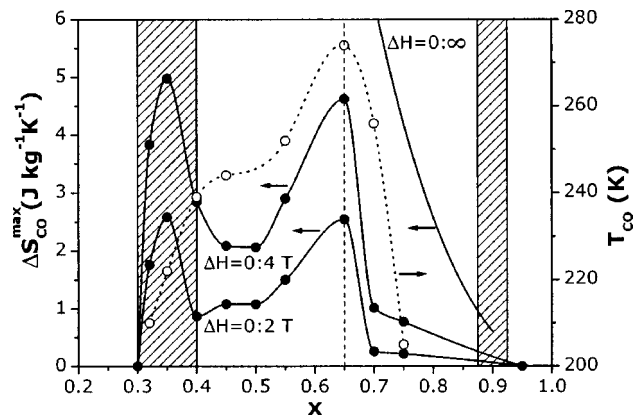


FIG. 7. Left axes: $\Delta S_{\text{CO}}^{\text{max}}$ as a function of Ca content x for $\Delta H = 2$ T, 4 T (estimated using experimental data) and ∞ [Eq. (14)]. See text for the meaning of $\Delta S_{\text{CO}}^{\text{max}}$. Right axes: charge-ordering temperature as a function of Ca content, x (open circles).

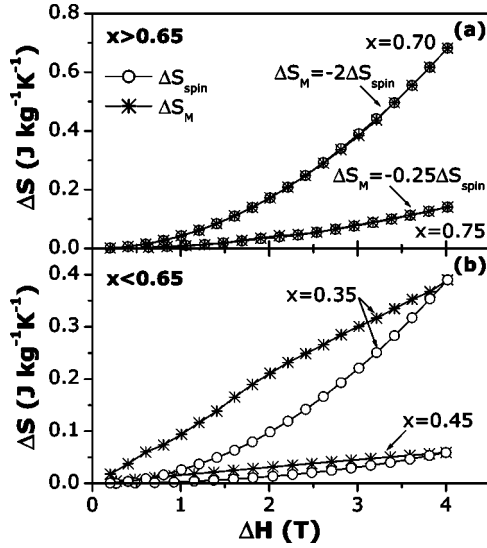


FIG. 8. Total magnetic entropy change ΔS_M and the spin contribution ΔS_{spin} as a function of the magnetic-field change ΔH , for (a) $x > 0.65$ and (b) $x < 0.65$. Results obtained for temperatures around the maximum of ΔS_M , analogously to $\Delta S_{\text{CO}}^{\text{max}}$.

shown in Fig. 8. These results were obtained for temperatures around the maximum of ΔS_M , analogously to $\Delta S_{\text{CO}}^{\text{max}}$. For $x > 0.65$ [Fig. 8(a)], the spin contribution ΔS_{spin} [Eq. (8)] has exactly the same tendency of the total magnetic entropy change ΔS_M , when analyzed as a function of magnetic-field change ΔH , with the following relations:

$$\Delta S_M = -2\Delta S_{\text{spin}}, \quad x = 0.70$$

$$\Delta S_M = -\frac{1}{4}\Delta S_{\text{spin}}, \quad x = 0.75. \quad (11)$$

Contrarily, for $x < 0.65$ [Fig. 8(b)], ΔS_{spin} increases with a different rate, comparing to ΔS_M . These interesting results lead us to conclude that for $x < 0.65$ there is more than one mechanism governing the charge ordering, including the magnetic order. On the other hand, for $x > 0.65$, only the alignment of the magnetic moments controls the charge ordering. This fact also explains the maximum in $T_{\text{CO}}(x)$, around $x \sim 0.65$, shown in Fig. 7 (present data) and Fig. 1 (literature data). Another work also analyzed the charge-ordering phase in terms of a interplay between the Jahn-Teller effect and magnetic ordering⁵² (and references therein).

An interesting aspect concerning the total magnetic entropy change, for several values of magnetic-field change, is the fact that it vanishes at the same temperature around T_{CO} , for any value of ΔH , as displayed in Fig. 9.

$\Delta S_{\text{CO}}^{\text{max}}$ can also be estimated, for $x > 0.65$, counting the number of accessible states Ω of the Mn^{3+} - Mn^{4+} ions, for two extreme cases: under zero field, i.e., with the maximum of charge ordering, since the nonaligned magnetic moments (paramagnetic phase) do not destroy the charge ordering; and under infinite field, i.e., with null charge ordering, since a completely aligned magnetic moments maximize the Mn^{3+} - Mn^{4+} electron hopping, destroying the charge order-

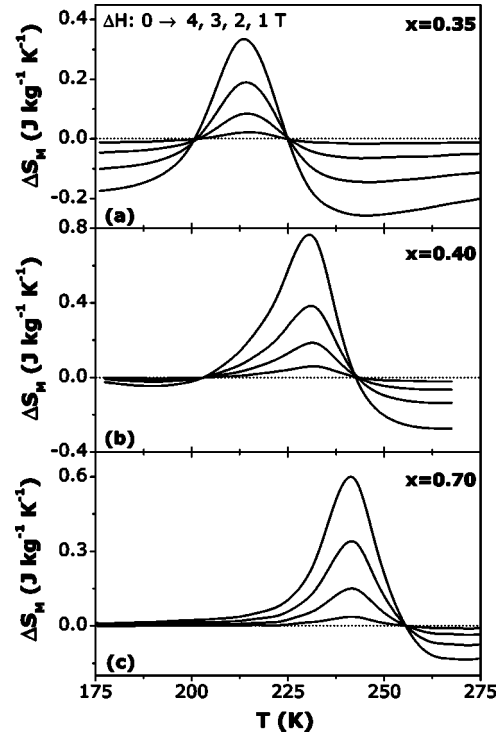


FIG. 9. Magnetic entropy change as a function of temperature, for several values of magnetic-field change and (a) $x=0.35$, (b) $x=0.40$, and (c) $x=0.70$.

ing. Thus, the number of accessible states for both cases are, respectively,

$$\Omega_{\text{CO}}^0 = \frac{(N-n)!}{n!(N-2n)!}, \quad (12)$$

$$\Omega_{\text{CO}}^\infty = \frac{N!}{n!(N-n)!}, \quad (13)$$

where $n=N(1-x)$, for $x > 0.5$, and N is the total number of Mn ions in the system. Thus, from the Boltzmann entropy we could evaluate $\Delta S_{\text{CO}}^{0:\infty} = S_{\text{CO}}(\Omega_{\text{CO}}^\infty) - S_{\text{CO}}(\Omega_{\text{CO}}^0)$, yielding

$$\Delta S_{\text{CO}}^{0:\infty} = N[(2x-1)\ln(2x-1) - 2x\ln x] \quad (14)$$

The above result (drawn in Fig. 7), is in agreement with the previously presented estimate.

Another interesting aspect is referred to as the low temperature of the samples with phase coexistence ($0.30 < x \leq 0.40$). Curiously, ΔS_M vanishes exactly at T_0 , being highly negative (positive) for higher (lower) values of temperature. For $x=0.32$, for instance, ΔS_M reaches $-19.4 \text{ Jkg}^{-1}\text{K}^{-1}$ at 32 K, and $-13.4 \text{ Jkg}^{-1}\text{K}^{-1}$ at 14 K. Figure 10 shows these features for $x=0.32$, 0.35, and 0.40, under 4 T of magnetic field change. Finally, the temperature dependence of the magnetic entropy change has a usual tendency with respect to several values of magnetic field change, as presented in the inset of Fig. 10, for $x=0.32$ and $\Delta H: 0 \rightarrow 1, 2, 3$, and 4 T. Note that ΔS_M vanishes at T_0 for any value of ΔH . Re-

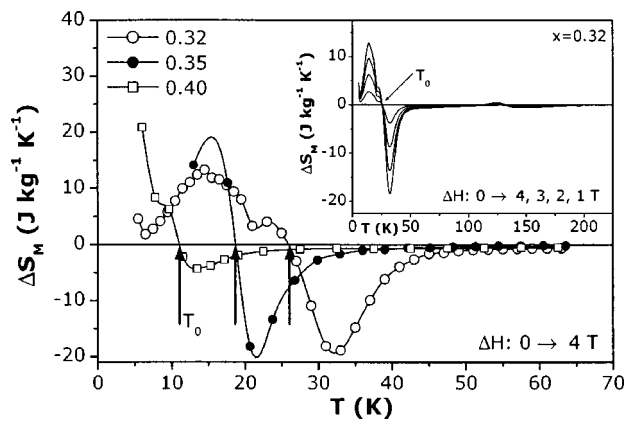


FIG. 10. Temperature dependence of the magnetic entropy change around T_0 , for $x=0.32$, 0.35 , and 0.40 , under 4 T of magnetic-field change. Inset: Idem, however, for several values of magnetic-field change and $x=0.32$.

cently, we published a detailed study of the low-temperature magnetic entropy change of these compounds ($0.30 < x \leq 0.40$).⁴⁶

V. CONCLUSION

In the present work we analyzed the magnetic entropy change ΔS_M for a wide range of Ca concentrations ($0.20 \leq x \leq 0.95$), covering several kinds of magnetic order. For

$x \leq 0.30$ and $x > 0.90$ we found an usual behavior for ΔS_M , since these samples have no charge-ordering. On the contrary, we found an anomalous magnetic entropy change for $0.30 < x < 0.90$ (concentrations exhibiting charge-ordering phenomenon), and the results could be explained considering a spin and charge-ordering contributions. In addition, taking some considerations into account, we could evaluate $\Delta S_{\text{CO}}^{\text{max}}$ as a function of Ca content x . From the analyzes of the magnetic entropy change as a function of the magnetic-field change ΔH , we could conclude that for $x < 0.65$ there is more than one mechanism governing the charge ordering, including the magnetic order, whereas for $x > 0.65$ only the alignment of the magnetic moments controls the charge ordering. Moreover, we found an extremely large value for the entropy variation at low temperatures (around T_0). Other manganites showing this characteristic temperature can also present a large magnetic entropy change, and, consequently, a great potential to be employed in various thermal devices.

ACKNOWLEDGMENTS

The authors thank FAPERJ/Brasil, FCT/Portugal (Contract No. POCTI/CTM/35462/99), GRICES/CAPES (Portugal-Brasil bilateral cooperation), and CTPETRO/CNPq/Brasil for financial support. M.S.R. acknowledges support from CNPq/Brasil. We are also thankful to J. S. Amaral and T. M. Mendonça, for their help with some magnetic measurements and sample preparation.

*Electronic address: marior@fis.ua.pt

- ¹V. K. Pecharsky and K. A. Gschneidner, *J. Appl. Phys.* **86**, 565 (1999).
- ²A. H. Morrish, *The Physical Principles of Magnetism* (Wiley, New York, 1965), Chap. 3.
- ³Y. Sun, W. Tong, N. Liu, and Y. Zhang, *J. Magn. Magn. Mater.* **238**, 25 (2002).
- ⁴P. Sande, L. E. Hueso, D. R. Miguens, J. Rivas, F. Rivadulla, and M. A. Lopez-Quintela, *Appl. Phys. Lett.* **79**, 2040 (2001).
- ⁵Y. Sun, X. Xu, and Y. Zhang, *J. Magn. Magn. Mater.* **219**, 183 (2000).
- ⁶Z. M. Wang, G. Ni, Q. Y. Xu, H. Sang, and Y. W. Du, *J. Appl. Phys.* **90**, 5689 (2001).
- ⁷G. Gu, J. Cai, W. Yang, and Y. Du, *J. Appl. Phys.* **84**, 3798 (1998).
- ⁸X. X. Zhang, J. Tejada, Y. Xin, G. F. Sun, K. W. Wong, and X. Bohigas, *Appl. Phys. Lett.* **69**, 3596 (1996).
- ⁹M. S. Reis, J. C. C. Freitas, M. T. D. Orlando, A. M. Gomes, A. L. Lima, I. S. Oliveira, A. P. Guimaraes, and A. Y. Takeuchi, *J. Magn. Magn. Mater.* **242**, 668 (2002).
- ¹⁰Y. Xu, U. Memmert, and U. Hartmann, *J. Magn. Magn. Mater.* **242**, 698 (2002).
- ¹¹P. Chen, Y. W. Du, and G. Ni, *Europhys. Lett.* **52**, 589 (2000).
- ¹²J. Mira, J. Rivas, L. E. Hueso, F. Rivadulla, and M. A. López-Quintela, *J. Appl. Phys.* **91**, 8903 (2002).
- ¹³L. E. Hueso, P. Sande, D. R. Miguéns, J. Rivas, F. Rivadulla, and M. A. López-Quintela, *J. Appl. Phys.* **91**, 9943 (2002).

- ¹⁴D. T. Morelli, A. M. Mance, J. V. Mantese, and A. L. Micheli, *J. Appl. Phys.* **79**, 373 (1996).
- ¹⁵A. Szweczyk, H. Szymczak, A. Wisniewski, K. Piotrowski, R. Kartaszynski, B. Dabrowski, S. Kolesnik, and Z. Bukowski, *Appl. Phys. Lett.* **77**, 1026 (2000).
- ¹⁶Z. B. Guo, Y. W. Du, J. S. Zhu, H. Huang, W. P. Ding, and D. Feng, *Phys. Rev. Lett.* **78**, 1142 (1997).
- ¹⁷H. Huang, Z. B. Guo, D. H. Wang, and Y. W. Du, *J. Magn. Magn. Mater.* **173**, 302 (1997).
- ¹⁸X. Bohigas, J. Tejada, E. del Barco, X. X. Zhang, and M. Sales, *Appl. Phys. Lett.* **73**, 390 (1998).
- ¹⁹X. Bohigas, J. Tejada, M. L. Marínez-Sarrión, S. Tripp, and R. Black, *J. Magn. Magn. Mater.* **208**, 85 (2000).
- ²⁰Y. Tokura and Y. Tomioka, *J. Magn. Magn. Mater.* **200**, 1 (1999).
- ²¹F. Millange, S. deBrion, and G. Chouteau, *Phys. Rev. B* **62**, 5619 (2000).
- ²²A. K. Raychaudhuri, A. Guha, I. Das, R. Rawat, and C. N. R. Rao, *Phys. Rev. B* **64**, 165111 (2001).
- ²³V. Hardy, A. Wahl, C. Martin, and C. Simon, *Phys. Rev. B* **63**, 224403 (2001).
- ²⁴M. R. Lees, O. A. Petrenko, G. Balakrishnan, and D. M. Paul, *Phys. Rev. B* **59**, 1298 (1999).
- ²⁵Z. Jirak, J. Hejtmanek, E. Pollert, and M. Marysko, *J. Appl. Phys.* **81**, 5790 (1997).
- ²⁶C. Martin, A. Maignan, M. Hervieu, and B. Raveau, *Phys. Rev. B* **60**, 12 191 (1999).
- ²⁷Y. Tomioka, A. Asamitsu, H. Kuwahara, Y. Moritomo, and Y.

- Tokura, *Phys. Rev. B* **53**, R1689 (1996).
- ²⁸Y. Tokura, Y. Tomioka, H. Kuwahara, A. Asamitsu, Y. Moritomo, and M. Kasai, *J. Appl. Phys.* **79**, 5288 (1996).
- ²⁹J. P. Renard and A. Anane, *Mater. Sci. Eng., B* **63**, 22 (1999).
- ³⁰Z. Jiráček, S. Krupicka, Z. Simsa, M. Dlouhá, and S. Vratislav, *J. Magn. Magn. Mater.* **53**, 153 (1985).
- ³¹M. S. Reis, V. S. Amaral, P. B. Tavares, A. M. Gomes, A. Y. Takeuchi, A. P. Guimaraes, I. S. Oliveira, and P. Panissod, *cond-mat/0211143* (unpublished).
- ³²D. E. Cox, P. G. Radaelli, M. Marezio, and S. W. Cheong, *Phys. Rev. B* **57**, 3305 (1998).
- ³³C. Frontera, J. L. García-Muoz, A. Llobet, M. Respaud, J. M. Broto, J. S. Lord, and A. Planes, *Phys. Rev. B* **62**, 3381 (2000).
- ³⁴M. Roy, J. F. Mitchell, A. P. Ramirez, and P. Schiffer, *Phys. Rev. B* **62**, 13 876 (2000).
- ³⁵M. Roy, J. F. Mitchell, A. P. Ramirez, and P. Schiffer, *Philos. Mag. B* **81**, 417 (2001).
- ³⁶M. M. Savosta, P. Novák, M. Marysko, Z. Jiráček, J. Hejtmánek, J. Englich, J. Kohout, C. Martin, and B. Raveau, *Phys. Rev. B* **62**, 9532 (2000).
- ³⁷J. Rivas, L. E. Hueso, A. Fondado, F. Rivadulla, and M. A. López-Quintela, *J. Magn. Magn. Mater.* **221**, 57 (2000).
- ³⁸P. Levy, F. Parisi, G. Polla, D. Vega, G. Leyva, H. Lanza, R. S. Freitas, and L. Ghivelder, *Phys. Rev. B* **62**, 6437 (2000).
- ³⁹L. E. Hueso, F. Rivadulla, R. D. Sánchez, D. Caeiro, C. Jardón, C. Vázquez-Vázquez, J. Rivas, and M. A. López-Quintela, *J. Magn. Magn. Mater.* **189**, 321 (1998).
- ⁴⁰J. F. Mitchell, D. N. Argyriou, C. D. Potter, D. G. Hinks, J. D. Jorgensen, and S. D. Bader, *Phys. Rev. B* **54**, 6172 (1996).
- ⁴¹J. Alonso, E. Herrero, J. M. Gonzalez-Calbet, M. Vallet-Regi, J. L. Martinez, J. M. Rojo, and A. Hernando, *Phys. Rev. B* **62**, 11 328 (2000).
- ⁴²H. L. Ju and H. Sohn, *J. Magn. Magn. Mater.* **167**, 200 (1997).
- ⁴³S. V. Trukhanov, I. O. Troyanchuk, F. P. Korshunov, V. A. Sirenko, H. Szymczak, and K. Baerner, *J. Low Temp. Phys.* **27**, 283 (2001).
- ⁴⁴G. Allodi, R. DeRenzi, and G. Guidi, *Phys. Rev. B* **57**, 1024 (1998).
- ⁴⁵C. Vazquez-Vazquez, M. C. Blanco, M. Lopez-Quintela, R. D. Sanchez, J. Rivas, and S. B. Oseroff, *J. Mater. Chem.* **8**, 991 (1998).
- ⁴⁶A. M. Gomes, F. Garcia, A. P. Guimaraes, M. S. Reis, and V. S. Amaral, *Appl. Phys. Lett.* **85**, 4974 (2004).
- ⁴⁷M. R. Lees, J. Barratt, G. Balakrishnan, D. M. Paul, and C. Ritter, *Phys. Rev. B* **58**, 8694 (1998).
- ⁴⁸H. Yoshizawa, H. Kawano, Y. Tomioka, and Y. Tokura, *Phys. Rev. B* **52**, 13 145 (1995).
- ⁴⁹S. Angappane, M. Pattabiraman, G. Rangarajan, K. Sethupathi, and V. S. Sastry, *Phys. Rev. B* **69**, 094437 (2004).
- ⁵⁰F. Dupont, S. deBrion, F. Millange, and G. Chouteau, *Appl. Magn. Reson.* **19**, 485 (2000).
- ⁵¹A. Kumar, N. Ghosh, J. P. Joshi, H. L. Bhat, and S. V. Bhat, *Solid State Commun.* **123**, 379 (2002).
- ⁵²S. Uhlenbruck, R. Teipen, R. Klingeler, B. Büchner, O. Friedt, M. Hücker, H. Kierspel, T. Niemöller, L. Pinsard, A. Revcolevschi, and R. Gross, *Phys. Rev. Lett.* **82**, 185 (1999).